(4) Heiszwolf, G. J.; Kloosterziel, H. *Recl. Trav. Chim. Pays-Bas* **1970**, *89*, 1217–1228.
(5) Cuvigny, T.; Larchevêque, M.; Normant, H. *Justus Liebigs Ann. Chem* **1975**, 719–730.
(6) Knorr, R.; Weiss, A.; Polzer, H. *Tetrahedron Lett.* **1977**, 459–462.
(7) Corey, E. J.; Enders, D.; Bock, M. G. *Tetrahedron Lett.* **1976**, 7–10. Le-Borgne, J. F. *J. Organomet. Chem.* **1976**, *122*, 139–143.
(8) Ahlbrecht, H.; Liesching, D. *Synthesis* **1976**, 746–748. DeJeso, B.; Pommier, J. C. *J. Organomet. Chem.* **1976**, *122*, C1–C5.
(9) (a) Meyers, A. I.; Poindexter, G. S.; Brich, Z. *J. Org. Chem.* **1978**, *43*, 892–898. (b) Meyers, A. I.; Williams, D. R. *Ibid.* **1978**, *43*, 3245–3247.
(10) Hoobler, M. A.; Bergbreiter, D. E.; Newcomb, M. *J. Am. Chem Soc.* **1978**, *100*, 8182–8185. Meyers, A. I.; Snyder, E. S.; Ackerman, J. J. H. *Ibid.* **1978**, *100*, 8186–8189.
(11) Ahlbrecht, H.; Düber, E. O.; Enders, D.; Eichenauer, H.; Weuster, P. *Tetrahedron Lett.* **1978**, 3691–3694.
(12) Cuvigny, T.; Normant, H.; Hullot, P. *Bull. Soc. Chim. Fr.* **1970**, 3976–3980.
(13) DeJeso, B.; Pommier, J. C. *J. Chem. Soc., Chem. Commun.* **1977**, 565–566; *J. Organomet. Chem.* **1977**, *137*, 23–29.
(14) Ahlbrecht, H.; Fischer, S. *Tetrahedron* **1973**, *29*, 659–664.
(15) The characteristic ^{1}H NMR chemical shifts of the olefinic β protons can be observed in nondeuterated THF (δ values given in ppm): **2a**, 5.03 (q); **3a**, 5.36 (q); **4a**, 5.40 (q); **5a**, 5.52 (q); **2b**, 5.45 (s); **3b**, 5.16 (s); **4b**, 6.37 (s); **5b**, 5.82 (s); **2c**, 3.60 (dt, ^3J = 13 Hz); **4c**, 4.22 (dt, ^3J = 13.5 Hz); **2d**, 4.50 (q); **3d**, 4.62 (q); **4d**, 4.98 (q); **5d**, 4.90 (q); **2e**, 4.43 (t); **3e**, 4.50 (t); **4e**, 5.00 (t); **5e**, 4.80 (t).
(16) Ahlbrecht, H.; Papke, G. *Tetrahedron* **1974**, *30*, 2571–2575.
(17) The enamines **4a** and **5a** derived from **1a** may be the actual catalysts.
(18) The empirical estimation of *E*/*Z* equilibrium constants will subsequently be published. Parts 4 and 5 of this series: *Chem. Ber.*, in press.
(19) Davenport, K. G.; Eichenauer, H.; Enders, D.; Newcomb, M.; Bergbreiter, D. E. *J. Am. Chem. Soc.* **1979**, *101*, 5654–5659.
(20) Fraser, R. R.; Banville, J.; Dhawan, K. L. *J. Am. Chem. Soc.* **1978**, *100*, 7999–8001.

Rudolf Knorr,* Peter Löw
Institute of Organic Chemistry, University of Munich
Karlstr. 23, D-8000 Munich 2, West Germany
Received November 5, 1979

Synthesis and Characterization of New Fe–Pd and Fe–Pt Carbonyl Anionic Clusters

Sir:

Mixed-metal carbonyl clusters may be useful as starting materials to generate bimetallic crystallites and, furthermore, may provide some insight in their behavior. Since recent work on alloy catalysts pointed out that in heterogeneous catalysis both selectivity and activity may be greatly affected by alloying,[1] extension of the range of known mixed-metal carbonyl clusters[2,3] is desirable.

We report here our preliminary results on the synthesis and characterization of a series of new Fe–Pd and Fe–Pt carbonyl anionic clusters, viz., $[Fe_4M(CO)_{16}]^{2-}$ (M = Pd, Pt), $[Fe_6Pd_6(CO)_{24}H]^{3-}$, and $[Fe_6Pd_6(CO)_{24}]^{4-}$. The two $[Fe_4M(CO)_{16}]^{2-}$ (M = Pd, Pt) dianions have been isolated in high yields (70–80%) as trimethylbenzylammonium (TMBA) salts from the reaction under nitrogen of $[TMBA]_2[Fe_3(CO)_{11}]$ with M(II) salts [MCl_2, K_2MCl_4, $(PhCN)_2MCl_2$, or $(SEt_2)_2MCl_2$] in a 1:0.7 molar ratio. The reaction follows the apparent stoichiometry

$$3[Fe_3(CO)_{11}]^{2-} + 2M^{2+} \xrightarrow{CH_3CN,\ 25\ °C} 2[Fe_4M(CO)_{16}]^{2-} + Fe^{2+} + CO \quad (1)$$

M = Pd, Pt

and, in both cases, the molar ratio is rather critical. Thus, when the amount of Pt(II) salts is increased, the initially formed $[Fe_4Pt(CO)_{16}]^{2-}$ is rapidly converted into a series of more oxidized Fe–Pt carbonyl anions, viz., $[Fe_3Pt_3(CO)_{15}]^{2-}$ and $[Fe_4Pt_6(CO)_{22}]^{2-}$. This reaction is presently under investigation.[4]

On the contrary, in the case of palladium, addition of excess Pd(II) salts results mainly in oxidation of the initially formed $[Fe_4Pd(CO)_{16}]^{2-}$ to $Fe(CO)_5$ and palladium metal, and there is no evidence of the intermediate formation of the corresponding Fe–Pd carbonyl anionic clusters.

Similar results have been obtained also using different polynuclear carbonyl ferrates, e.g., $[Fe_2(CO)_8]^{2-}$ and $[Fe_4(CO)_{13}]^{2-}$, as starting materials. However, slow reaction (5–10 days) of $[TMBA]_2[Fe_4(CO)_{13}]$ with K_2PdCl_4 (1:1 molar ratio) in THF affords a dark suspension; the red-brown solution contains mainly $Fe(CO)_5$, $[Fe_4(CO)_{13}H]^-$, $[Fe_4Pd(CO)_{16}]^{2-}$, and unreacted $[Fe_4(CO)_{13}]^{2-}$, whereas the dark precipitate (mostly KCl, Fe, and Pd metals) contains small amounts of a mixture of $[TMBA]_4[Fe_6Pd_6(CO)_{24}]$ and $[TMBA]_3[Fe_6Pd_6(CO)_{24}H]$. Although the yields of these two new products are generally very low (5–10%), the synthesis under these experimental conditions is reproducible, and the stabilization of these two more-oxidized Fe–Pd carbonyl anions is probably the result of the poor solubility in THF of their TMBA salts as well as of K_2PdCl_4. The two salts are slightly more soluble in acetone, acetonitrile, or dimethyl sulfoxide and are reversibly related by the equilibrium

$$[Fe_6Pd_6(CO)_{24}H]^{3-} \underset{CH_3CN}{\overset{Me_2SO}{\rightleftharpoons}} [Fe_6Pd_6(CO)_{24}]^{4-} + H^+ \quad (2)$$

Thus, dissolution either of the mixture or of the hydride derivative in Me_2SO slowly gives rise to formation of the brown $[Fe_6Pd_6(CO)_{24}]^{4-}$, which has been isolated in the solid state by addition of excess $TMBA^+Cl^-$ and water. On the contrary, controlled addition of phosphoric acid either to the mixture or to the pure tetraanion in CH_3CN results in separation of tiny black crystals of the less soluble $[TMBA]_3[Fe_6Pd_6(CO)_{24}H]$. All of these compounds are diamagnetic and their infrared spectra are reported in Table I.

Table I. Infrared Carbonyl Absorptions of the Fe–Pd and Fe–Pt Clusters in CH_3CN Solution

compd	color	ν_{CO}, cm^{-1}
$[Fe_4Pd(CO)_{16}]^{2-}$	brown	2035 (vw), 1980 (s), 1970 (s), 1960 (sh), 1940 (ms), 1910 (sh), 1850 (w, br)
$[Fe_4Pt(CO)_{16}]^{2-}$	brown	2020 (vw), 1985 (s), 1970 (s), 1960 (sh), 1935 (ms), 1925 (sh), 1830 (w, br)
$[Fe_6Pd_6(CO)_{24}]^{4-}$	brown	1980 (s), 1950 (sh), 1920 (sh), 1820 (sh), 1800 (m)
$[Fe_6Pd_6(CO)_{24}H]^{3-}$	green-brown	2005 (s), 1985 (m), 1950 (mw), 1840 (sh), 1825 (m)[a]

[a] Very weak ^{1}H NMR signal in acetone at τ 28.1.

The correct stoichiometry and the molecular structures of $[TMBA]_2[Fe_4Pd(CO)_{16}]$, $[TMBA]_2[Fe_4Pt(CO)_{16}]$, and $[TMBA]_3[Fe_6Pd_6(CO)_{24}H]\cdot 2CH_3CN$ have been ascertained by X-ray crystallography.[5,6] The structures of the two $[Fe_4M(CO)_{16}]^{2-}$ (M = Pd, Pt) dianions are substantially identical and derive from two $Fe_2(CO)_8$ moieties joined either to a central palladium or platinum atom to give rise to a rectangularly distorted square-planar coordination of iron atoms around the unique central metal atom. When M = Pd (Figure 1), all of the five metal atoms are virtually coplanar, while, when M = Pt, the two Fe_2Pt triangles are slightly twisted and form a dihedral angle of ~7°. Of the four carbonyl groups bonded to each iron atom, three are terminal, while the fourth is bent toward the central metal atom and is better described as semibridging.[8,9] Since this occurs alternately above and below the metal plane, the four semibridging carbonyl groups give rise to a superimposed tetrahedral coordination of carbon atoms around the central atom. This particular ligand arrangement is not only the result of steric factors,[10] but has also

0002-7863/80/1502-3242$01.00/0

Table II. Average Bonding Distances in the $[Fe_4M(CO)_{16}]^{2-}$ (M = Pd, Pt) and $[Fe_6Pd_6(CO)_{24}H]^{3-}$ Anions[a,b]

	$[Fe_4Pt(CO)_{16}]^{2-}$	$[Fe_4Pd(CO)_{16}]^{2-}$	$[Fe_6Pd_6(CO)_{24}H]^{3-}$
Fe-Fe	2.708	2.736	
Fe-M	2.601	2.599	2.698,[c] 2.609[d]
Pd-Pd			2.810,[c] 2.948[d]
Fe-C_t	1.765	1.742	1.742
C_t-O	1.15	1.17	1.17
Fe-C_{db}	1.814	1.766	1.841
C_{db}-O	1.16	1.18	1.19
M-C_{db}	2.285	2.371	2.106
Fe-C_{tb}			1.851
C_{tb}-O			1.19
M-C_{tb}			2.257
Fe··Fe	4.421	4.445	3.604

[a] Distances are given in ångstroms. [b] Typical esd's on single distances follow: Fe-M and Pd-Pd, 0.001; Fe-Fe, 0.002; Fe-C and M-C, 0.01; C-O, 0.02. [b] t = terminal; db = doubly bridging or semibridging; tb = triply bridging. [c] Within each Fe_3Pd_3 fragment. [d] Between the two Fe_3Pd_3 fragments.

an electronic origin. Thus, a comparison between the individual molecular parameters of the $[Fe_4M(CO)_{16}]^{2-}$ (M = Pd, Pt) dianions (Table II) shows a lengthening of 0.023 Å of the average Fe-C distance and a comparable shortening of the corresponding C-O and Fe-Fe bond distances on going from the palladium to the platinum derivative. This trend is in keeping with the presence of a decreased negative charge on the iron atoms when M = Pt and, conversely, of an increased negative charge on the central platinum atom, as shown also by the stronger interactions of platinum with the semibridging carbonyl groups, which are generally believed to favor charge equalization.[12,13]

The reluctance of palladium to bind CO, at least when dealing with isolated palladium atoms or small palladium clusters, is known.[15] The semibridging carbonyl groups found in $[Fe_4Pd(CO)_{16}]^{2-}$ suggest that a combination of steric and electronic factors, induced by incorporation of iron atoms in the cluster, may favor Pd-C interactions, but a yet better proof stems from the structure of the $[Fe_6Pd_6(CO)_{24}H]^{3-}$ trianion shown in Figure 2.

The metal skeleton of this dodecanuclear mixed-metal carbonyl anion does not have a precedent in either homo- or heterometallic molecular clusters and consists of a trigonal antiprismatic array of six palladium atoms with the six lateral faces capped by six iron atoms. Alternatively, this metal framework may also be obtained by bringing together along the C_3 axis and in a staggered conformation two quasi-planar Fe_3Pd_3 units which may be seen as slightly distorted fragments of two adjacent (111) layers of the face-centered cubic superstructure of the $FePd_3$ alloy.[16]

Of the 24 carbonyl groups, 12 are terminally bonded, two per iron atom, six are doubly bridging the six Fe-Pd bonds connecting the two Fe_3Pd_3 fragments, and six are triply

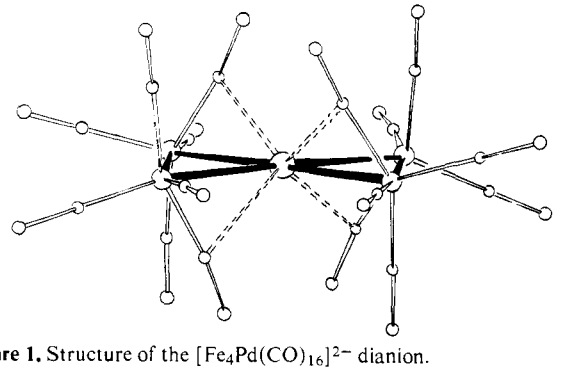

Figure 1. Structure of the $[Fe_4Pd(CO)_{16}]^{2-}$ dianion.

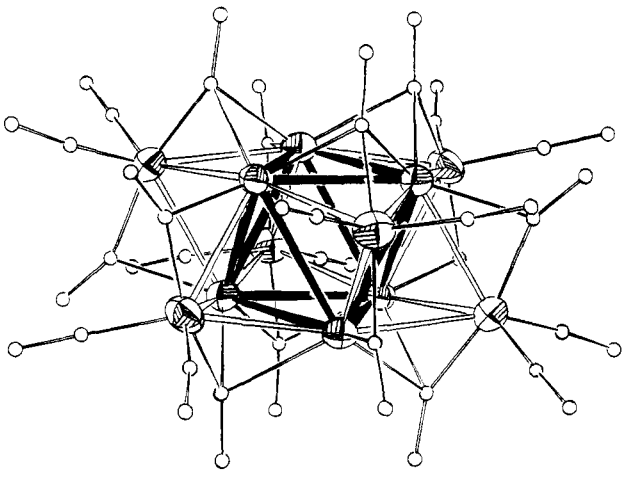

Figure 2. ORTEP drawing of $[Fe_6Pd_6(CO)_{24}H]^{3-}$. Blackened bonds emphasize the Pd_6 core.

bridging the six $FePd_2$ triangles of the two monolayers. Therefore, although the palladium atoms do not bind any terminal carbonyl ligand, each one of them is bonded to three different CO's and the Pd-C bonds in this case are shorter than in $[Fe_4Pd(CO)_{16}]^{2-}$ (Table II).

The hydride hydrogen atom has not been directly located by difference Fourier, and indirect evidence is elusive. Three types of coordination seem available: terminal on the palladium atoms, triply bridging on the Pd_3 triangle of each Fe_3Pd_3 monolayer, and interstitial in the Pd_6 octahedral cavity. Interstitial coordination would be supported by the unusually long average Pd-Pd distance (2.88 Å),[17] as well as by our unsuccessful attempts to further protonate the trianionic cluster. This last behavior reminds us of the interstitial $[Ni_{12}(CO)_{21}H_{4-n}]^{n-}$ (n = 2, 3),[20] which cannot be further protonated once both the two octahedral cavities have been occupied.

Acknowledgment. We acknowledge Professor P. Chini for continuous interest and helpful suggestions.

Supplementary Material Available: A listing of the thermal and positional parameters of $[N(CH_3)_3CH_2Ph]_2[Fe_4Pt(CO)_{16}]$ (Table III), $[N(CH_3)_3CH_2Ph]_2[Fe_4Pd(CO)_{16}]$ (Table IV), and $[N(CH_3)_3CH_2Ph]_3[Fe_6Pd_6(CO)_{24}H]\cdot 2CH_3CN$ (Table V) (4 pages). Ordering information is given on any current masthead page.

References and Notes

(1) Sinfelt, J. H. *Prog. Solid State Chem.* **1975**, *10*, 55-69.
(2) Calderazzo, F.; Ercoli, R.; Natta, G. In "Organic Chemistry via Metal Carbonyls", Wender, I., Pino, P., Eds.; Interscience: New York, 1978; Vol 1, pp 256-272.
(3) Gladfelter, W. L.; Geoffroy G. L. *Adv. Organomet. Chem.*, in press.
(4) Longoni, G.; Manassero, M.; Sansoni, M., work in progress.
(5) Crystal and analytical data follow. $[TMBA]_2[Fe_4Pd(CO)_{16}]$: M = 1077.8; $TMBA^+$:Fe:Pd:CO, 1.97:4.03:1.0:15.5 (calcd 2:4:1:16); triclinic; space group $P\bar{1}$; a = 11.974 (2), b = 18.310 (4), c = 11.559 (3) Å; α = 105.51 (3), β = 118.14 (2), γ = 92.53 (3)°; V = 2109 Å^3; D_m = 1.69 (2), D_c = 1.69 g/cm^3 for Z = 2. The current R for 4100 independent reflections having $\sigma(I)/I \leq 0.25$ is 0.048. $[TMBA]_2[Fe_4Pt(CO)_{16}]$: M = 1166.5; $TMBA^+$:Fe:Pt:CO, 1.98:3.92:1.0:15.8 (calcd 2:4:1:16); monoclinic; space group C_2/c (after refinement); a = 19.100 (4), b = 15.139 (3), c = 20.511 (8) Å; β = 132.30 (2)°; V = 4384.9 Å^3; D_m = 1.76 (2), D_c = 1.75 g/cm^3 for Z = 4. The anion lies on a crystallographic twofold axis which bisects the two Fe–Fe bonds and passes through the platinum atom. The current R for 2414 independent reflections having $\sigma(I)/I \leq 0.25$ is 0.039. $[TMBA]_3[Fe_6Pd_6(CO)_{24}H]\cdot 2CH_3CN$: M = 2179.6; $TMBA^+$:Fe:Pd, 0.54:0.95:1.0 (calcd 0.5:1:1); hexagonal; space group $P6_3/m$ (after refinement); a = 13.182 (3), c = 23.613 (6) Å; V = 3553.3 Å^3; D_c = 2.04 g/cm^3 for Z = 2. The anion has crystallographic $3(S_6)$ and idealized $3m(D_{3d})$ site symmetry. The current R for 893 independent reflections having $I \geq 4\sigma(I)$ is 0.032. Intensities were collected on a BASIC diffractometer[7] with graphite monochromatized Mo Kα radiation up to 2ϑ = 50°. The structures have been solved by standard Patterson and Fourier methods and refined by block-matrix least squares to the current R's.
(6) For computation of distances and bond angles, see paragraph at the end of the paper regarding supplementary material.
(7) Casella, L.; Gullotti, M.; Pasini, A.; Ciani, G.; Manassero, M.; Sironi, A. *Inorg. Chim. Acta* **1978**, *26*, L1-L2.
(8) The average Fe-C-O angle of the semibridging carbonyl groups is 163.0°

when M = Pt and 166.8° when M = Pd, whereas the corresponding terminal carbonyl groups show an average angle of 177.7 and 175.8°, respectively.
(9) Cotton, F. A. *Prog. Inorg. Chem.* **1977**, *21*, 1–28.
(10) In the related $Sn[Fe_2(CO)_8]_2$ derivative, the shortest Sn·C contacts are longer than 3.0 Å.[11]
(11) Lindley, P. F.; Woodward, P. *J. Chem. Soc. A* **1967**, 382–392.
(12) Chini, P.; Ciani, G.; Garlaschelli, L.; Manassero, M.; Martinengo, S.; Sironi, A.; Canziani, F. *J. Organomet. Chem.* **1978**, *152*, C35–C38.
(13) This difference in charge distribution in the $[Fe_4M(CO)_{16}]^{2-}$ (M = Pd, Pt) dianions is in agreement with Pauling electronegativities of the metals. Electron transfer from iron to platinum has been previously inferred from Mossbauer isomer shift in Fe–Pt Alloys.[14]
(14) Vannice, M. A.; Garten, R. L. *J. Mol. Catal.* **1975–1976**, *1*, 201–222.
(15) Longoni, G.; Chini, P. *J. Am. Chem. Soc.* **1976**, *98*, 7225–7231, and references therein.
(16) Hultgren, R.; Zapffe, C. A. *Zeit. Krist.*, **1938**, *99*, 511.
(17) Comparable values are 2.75 Å for palladium metal, 2.582 Å for $Mo_2Pd_2Cp_2(CO)_8(PEt_3)_2$,[18] and 2.89 Å for the $PdH_{0.7}$ phase.[19]
(18) Bender, R.; Braunstein, P.; Dusasoy, Y.; Protas, J. *Angew. Chem., Int. Ed. Engl.* **1978**, *17*, 596–597.
(19) MacKay, K. M. In "Comprehensive Inorganic Chemistry"; Pergamon: London, 1973; Vol. 1, p 23.
(20) Broach, R. W.; Dahl, L. F.; Longoni, G.; Chini, P.; Schultz, A. J.; Williams, J. M. *Adv. Chem. Ser.* **1978**, No. 167, 93–110.

Giuliano Longoni*
Centro del CNR per lo studio della sintesi e della struttura dei composti dei metalli di transizione via G. Venezian 21, 20133 Milan, Italy

Mario Manassero, Mirella Sansoni
Istituto di Chimica Generale dell'Università di Milano via G. Venezian 21, 20133 Milan, Italy

Received May 21, 1979

Models for Nicotinamide Coenzymes. Isotope Effect Discrepancies in the Reaction of Dihydronicotinamides with Trifluoroacetophenone Are Due to Adduct Formation

Sir:

Several years ago we suggested that the oxidation-reduction reaction of a 1,4-dihydronicotinamide (**1**) with trifluoroacetophenone (**2**) (Scheme I) proceeds via an intermediate.[1] This was based on our observation that isotope effects determined by comparison of the rates of disappearance of protio- and 4-deuteriodihydronicotinamides (**1** and **1**-d_1)[2] were small compared with those determined from the partitioning of hydrogen and deuterium from **1**-d_1 into the product phenyltrifluoroethanol (**4**). This discrepancy would be explained if there was a noncovalent intermediate on the reaction pathway, with the rate-determining step *preceding* the hydrogen transfer. Similar results were subsequently reported for other oxidations of dihydronicotinamides, and two-step mechanisms proposed for these reactions as well.[3] It now appears, however, that our conclusions were premature. In this report we demonstrate that the discrepancy in isotope effects is due to the reversible formation of a covalent adduct[4] **5** which is *not* on the pathway for the oxidation-reduction reaction (Scheme II).

Scheme I

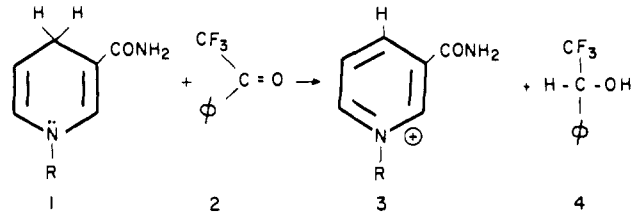

Scheme II

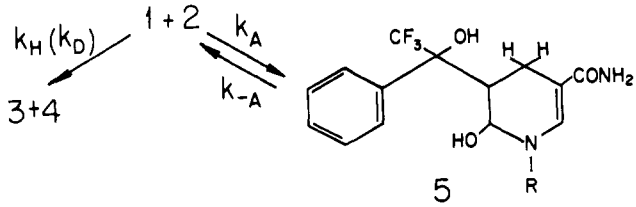

The isotope effects were remeasured for two dihydronicotinamides under conditions minimizing the complicating unimolecular (hydration) component[1] in the disappearance of **1**. In 0.1 M $NaHCO_3$–0.1 M Na_2CO_3 buffer, pH 9.9, in 25% 2-propanol at 50 °C, the disappearance of **1** (UV, 355 nm) in the presence of a large excess of **2** is pseudo first order, with $k_{obsd} = k_{app}[\mathbf{2}]$. The initial rates of disappearance of dihydronicotinamides[2,5] **1**, **1**-d_1, and **1**-d_2 were measured simultaneously in identical solutions of **2** so as to determine the relative rates (k_{HH}/k_{HD}, k_{HH}/k_{DD}; Table I, entries 2 and 3) with maximum accuracy. The relative rates of transfer of H and D from **1**-d_1 to **2**, k_H/k_D, were determined in the above medium by isotopic analysis of the product alcohol **4** (Table I, entry 4). Data were corrected for the isotopic compositions of the samples of **1** used.[6] To make certain that deuterium had not been lost by exchange with solvent, the reactions were repeated with $[^3H]$-H_2O in the medium and **4** isolated as the *p*-nitrobenzyl ester.[1b] Scintillation counting of the ester showed that <0.1% of the hydrogen on the carbinol carbon (H-C-O) of **4** was derived from the solvent. The data confirm our report of discrepancies in isotope effects.

We must now consider this data in the light of formation of **5**. The adduct **5a** (R = propyl) precipitated in 10–15% yield when a buffered (0.1 M carbonate, pH 9.9) solution *saturated* in **1a** and **2** was held at 40 °C and was shown to have the IR,

Table I. Kinetic and Isotope Effect Data for Reactions of Dihydronicotinamides **1** with Trifluoroacetophenone (**2**)[a]

entry		dihydronicotinamide (R) **1a** (*n*-propyl)	**1b** (benzyl)
1	k_{app}, M^{-1} min^{-1} [b]	0.207 ± 0.014[c]	0.065 ± 0.003[d]
2	k_{HH}/k_{HD} (rel rate)[b,e,f]	1.29 ± 0.04[c]	1.55 ± 0.15[d]
3	k_{HH}/k_{DD} (rel rate)[b,e,g]	1.93 ± 0.13[c]	2.19 ± 0.11[d]
4	k_H/k_D (product analysis)[e,h]	6.7 ± 1.8	6.6 ± 1.7
5	$2k_H/(2k_H + k_A)$ (calcd, eq 3)	0.57 ± 0.06	0.64 ± 0.05
6	$2k_H/(2k_H + k_A)$ (calcd, eq 4)	0.53 ± 0.07	0.84 ± 0.14
7	k_H, M^{-1} min^{-1} } constants for Scheme II[i]	0.06	0.02
8	k_A, M^{-1} min^{-1} } constants for Scheme II[i]	0.09	0.02
9	k_{-A}, min^{-1} } constants for Scheme II[i]	0.006	0.005

[a] All measurements were done at 50.0 ± 0.2 °C in 0.1 M $NaHCO_3$–0.1 M Na_2CO_3 buffer, pH 9.9, ionic strength 0.5, in 25% 2-propanol (v/v). [b] Disappearance of **1** followed spectrophotometrically at 355 nm. [c] Average from 21 experiments over the range of [**2**] from 0.025 to 0.2 M. [d] Average from 11 experiments, [**2**] = 0.05–0.2 M. [e] Corrected for isotopic composition of starting samples of **1**. [f] Relative k_{app} for **1** and **1**-d_1. [g] Relative k_{app} for **1** and **1**-d_2. [h] 0.01 M **1**-d_1 and 0.04 M **2** were incubated for 48 h (>95% completion); crude **4** was isolated and analyzed by mass spectroscopy (average from three experiments). [i] k_H and k_A were calculated from the ratio $2k_H/(2k_H + k_A)$ and the assumption that $2k_H + k_A = k_{app}$. k_{-A} was chosen to fit data for **4** formation (e.g., Figure 2).

0002-7863/80/1502-3244$01.00/0